Solar Observing

James R. Graham
2014/11/16

Telescope & optical fiber

A heliostat provides convenient delivery of a solar image to a stationary spectrograph. However, the cost of such a system was considered to be prohibitive. Instead, we chose to use an optical fiber at the focal plane of a surplus 10-cm, $F/10$ Newtonian telescope. The telescope drive is turned off and data are acquired using constant declination scans at the sidereal rate (15 cos $\delta_\odot$ arc seconds per second, where $-23.^\circ5 < \delta_\odot < 23.^\circ5$).

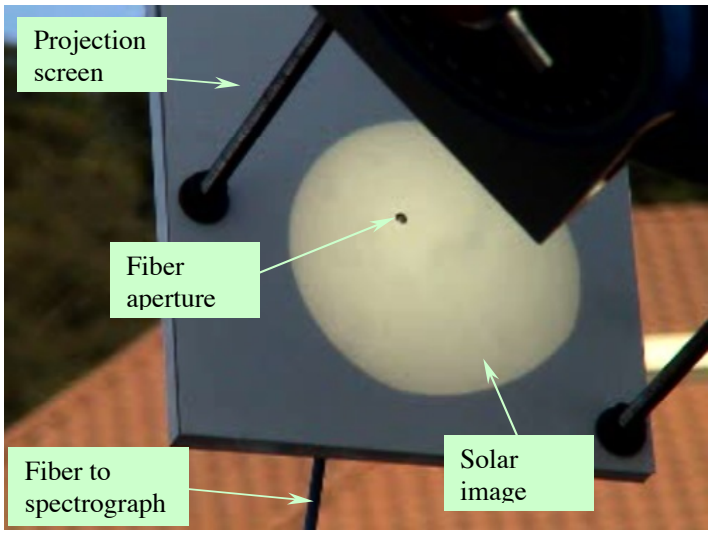

Figure 1: The solar transit telescope on the roof of the Astronomy Department feeding the echelle spectrograph. The telescope is stationary and the rotation of the earth scans the solar image across the fiber aperture. A movie of a transit may be viewed at http://ugastro.berkeley.edu/infrared/spectrum/index.html.

An optical fiber provides a convenient way to conduct light from the telescope focal plane to a stationary spectrograph (e.g., Barden 1995). Multimode fibers come in two distinct classes: step-index and graded index. Unlike step-index fibers, the value of the refractive index of the core of a graded index fiber varies continuously with distance from the center of the fiber. Step-index fibers have relatively large core diameters and large numerical apertures (NA), which makes them relatively easy to couple to astronomical instruments. Multimode, step-index fiber core sizes are typically 50 or 62.5 μm. Step-index fibers have limited bandwidth capabilities relative to graded-index fibers, due to modal dispersion, which means that graded-index fibers predominate in commercial telecommunications applications.

We choose a 50-μm diameter core step-index fiber (Corning InfiniCor), which gives an aperture size of 3.5 arc seconds when used at the focus of the solar telescope. The numerical aperture is 0.2, which is typical of silica fibers. The 25-m long fiber runs from a darkened lab to an adjacent parking ling where the telescope is deployed. The fiber is terminated with SMA 905 connectors, which provide accurate and reproducible location of the fiber tip in the focal planes of the telescope and the spectrograph.

Solar transit scan

In principle, the measurement of solar rotation could be made using a single observation of the Doppler shift of the solar limb at the equator. However, the details of the geometric arrangement of the solar system are complex and we need to consider the obliquity of the spin axes of the sun and the earth and the coordinate transformations necessary to identify locations on the projected solar disk. Even if we knew how to locate the solar equator this is not practical because our telescope does not point and track with accuracy or precision. Moreover, because of the phenomenon of limb darkening the surface of the solar limb is zero (in the Eddington approximation.) It is important be aware that there are errors in the wavelength scale and it is unlikely that our spectrometer can make absolute velocity measurements of sufficient accuracy for our purposes. These factors combine to explain why the only practical approach employs differential Doppler measurements derived from a drift scan across a solar diameter at constant declination.

Interpretation of the drift scan method requires some sophistication. Although this approach simplifies data collection, it requires reconstruction of the path of the fiber and interpretation of the results.

Coordinate Transformations

The obliquity (tilt of the spin axes) of the sun and the earth are 7.°25 and 23.°5, respectively. During the course of the earth's orbit the apparent position angle of the sun's rotation changes: it may be displaced by ±26.°5 relative to the solar meridian and tilted toward or away from the earth by ±7.°25. With reference to Figure 2 we introduce the transformation from some point **R** on the surface in a solar reference frame (x, y, z) to the terrestrial frame, defined by the angles (ξ, η).

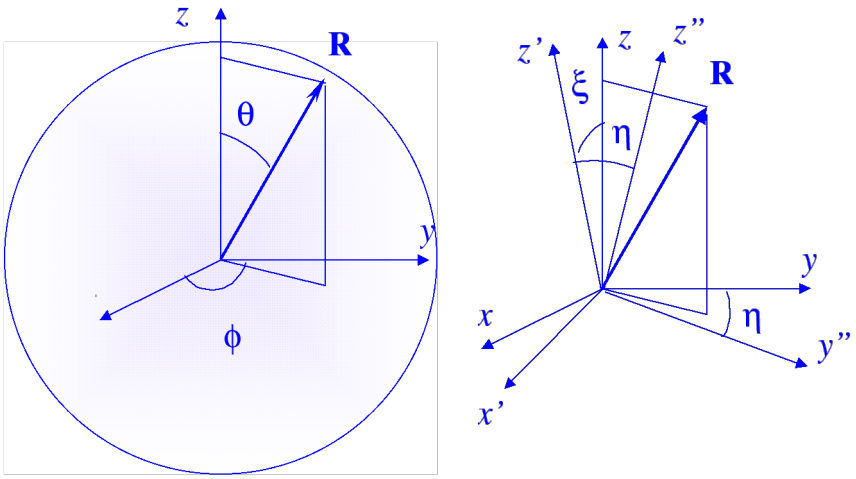

Figure 2: Solar geometry and transformation to the observed reference frame. In this example the plane of the sky is (*z*", *y*").

A point on the solar surface in Cartesian coordinates

$$\begin{aligned} x &= R\sin\theta\cos\phi \\ y &= R\sin\theta\sin\phi \\ z &= R\cos\theta \end{aligned} \tag{1}$$

has velocity

$$\begin{aligned} \dot{x} &= -R\sin\theta\sin\phi\dot{\phi} \\ \dot{y} &= R\sin\theta\cos\phi\dot{\phi} \\ \dot{z} &= 0 \end{aligned} \quad , \tag{2}$$

where $\dot{\phi}$ is the angular velocity. It is a straightforward exercise to construct the rotation matrices describing a rotation about the *y*-axis by the angle ξ followed by a rotation about the *x*'-axis by angle η to compute Cartesian components of **R** and $\dot{\mathbf{R}}$ in the observer's (*x*", *y*", *z*") frame and hence find radial velocity at any point on the solar disk.

The first step is to rotate about the y-axis by the angle ξ, which has the effect of tilting the solar spin axis towards the earth,

$$\begin{pmatrix} x' \\ y' \\ z' \end{pmatrix} = \begin{pmatrix} \cos\xi & 0 & \sin\xi \\ 0 & 1 & 0 \\ -\sin\xi & 0 & \cos\xi \end{pmatrix} \begin{pmatrix} x \\ y \\ z \end{pmatrix} \tag{3}$$

The second rotation rotates about the *x*'-axis by angle η, which changes the apparent orientation of the spin axis relative to north,

$$\begin{pmatrix} x'' \\ y'' \\ z'' \end{pmatrix} = \begin{pmatrix} 1 & 0 & 0 \\ 0 & \cos\eta & \sin\eta \\ 0 & -\sin\eta & \cos\eta \end{pmatrix} \begin{pmatrix} x' \\ y' \\ z' \end{pmatrix} \quad (4)$$

The angles (ξ, η) are conveniently tabulated by the JPL Horizons ephemeris for the sun (http://ssd.jpl.nasa.gov). At the time of the observation described below (2008 Dec 22 19:00 UT) the sun's spin axis position angle (measured counterclockwise with respect to direction of the celestial north pole) is 6.°42 and the apparent latitude of the center of the sun is –1.°92.

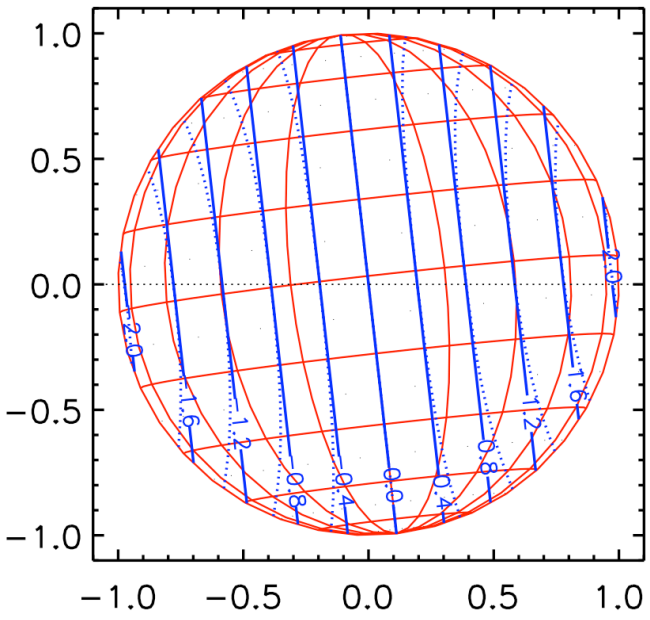

Figure 3: The apparent solar disk with lines of latitude and longitude at 18° increments for Dec 22 when the sun's north pole position angle was 6.°42 and the apparent latitude of the center of the disk was –1.°92. The coordinate system is celestial with north up and east to the left—(*y*", *z*") in the notation of Figure 2. The dotted horizontal line shows the trajectory of a drift scan that cuts the sun at a diameter. Straight blue contour lines are lines of constant radial velocity (km/s) for solid body rotation at the sidereal equatorial period (24.47 days). The dotted contours are for the differential rotation law of Snodgrass & Ulrich (1990) and illustrate the departure from solid-body rotation.

Figure 3 shows the velocity using the measured sidereal rotation period. Thus, the predicted velocities are those that would be recorded in an inertial frame. Assuming that the earth's orbit is circular, the observed velocity should be corrected for the components orbital motion the earth's spin along the line of sight.

Observations

The telescope is pointed to the declination of the center of the solar disk and oriented a few minutes west of the limb with the sidereal drive turned off. The control software for the Apogee camera is triggered and the CCD is read out at regular intervals during the duration of the transit. Pointing the telescope in declination is an iterative procedure that ensures that the transit scan cuts the sun at a diameter—other scans can be employed but reconstruction of the trajectory requires more work. A target drawn on the eyepiece projection screen with diameter equal to that of the solar disk is used for coarse alignment and then the telescope is offset in hour angle to the west to demonstrate that sidereal rotation carries the fiber in a path that is tangential to the limb. If the telescope polar axis has been aligned, scanning in hour angle by hand accelerates this step.

A solar observation set comprises a time series of spectra. An exposure time of 20 ms gives peak counts of about half full well; the CCD is windowed in the y-direction so that 1024×100 pixels are read out and mean interval between exposures is 8.8 seconds. This results in 14 to 16 spectra of the sun at the autumnal equinox and winter solstice, respectively.

Figure 4 shows a solar spectrum collected using the telescope configuration shown in Figure 1 with a 633 nm, 10 nm-wide blocking filter. This is the average of 14 individual spectra collected during a two-minute solar drift scan. Figure 1 shows that fiber input is not well baffled from ambient light, so the observations should be corrected for scattered sunlight by subtracting frames acquired with the solar image off the fiber aperture. The data are flat fielded using a quartz-halogen lamp that illuminates the fiber. Figure 4 also displays the McMath-Pierce FTS solar spectrum. The only correction applied to make is this comparison involves smoothing the FTS data to our resolution with a Gaussian kernel. The close resemblance confirms that solar spectra can be recorded with good accuracy and precision and that the wavelength scale is consistent. Order 35 was chosen only because it coincides with the 632.8 nm HeNe line, but it has strong, sharp features that are suitable for Doppler measurements.

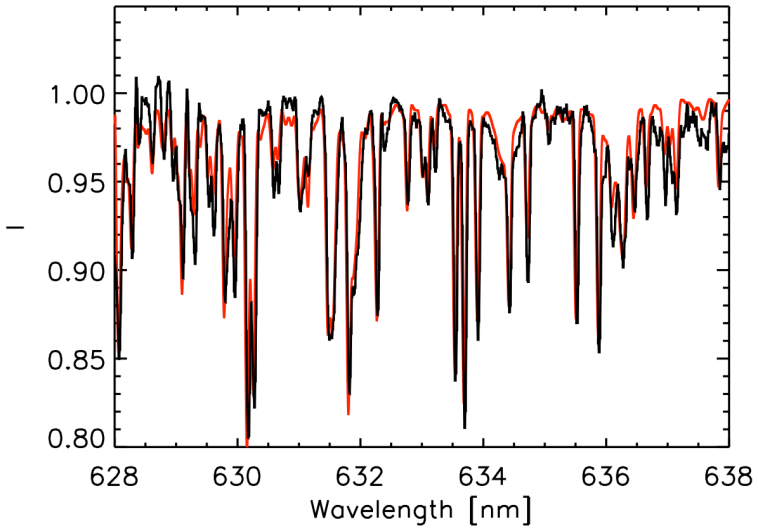

Figure 4: The solar spectrum (black) from echelle order 35 selected using the 633 nm order-sorting filter. This spectrum shows that order 35 has plenty of sharp features for Doppler measurements. The McMath Pierce FTS solar spectrum (red), smoothed to the same resolution is overplotted.

Limb darkening

The total intensity versus time recorded in a typical scan is shown in Figure 5. This plot provides a convenient check on the integrity of the data—intensity fluctuations indicate the presence of cloud or buffeting of the telescope by wind or by the observers. Both are undesirable: the former causes additional scattered light that will dilute the Doppler signature and the latter implies pointing errors that will introduce systematic errors. The time series of total intensity also provides a practical demonstration of limb darkening.

The observed brightness, *I*, of any point on the surface of a star is predicted by the Eddington approximation for a grey, plane parallel atmosphere to be

$$I = I_0 \frac{2 + 3\cos\theta}{5} \tag{5}$$

where θ is the angle between the line of sight and the vector normal to the surface of the star, i.e., $\theta = 0$ at the center of the solar disk and $\theta = \pi/2$ at the edge.

If we observe a position on the sun that is at a projected distance *r* from the center solar disk, then $r = R\sin\theta$. For a sequence of observations at time *t* then $r/R = (t - t_0)/\Delta t$, if t_0 is the time when center of the sun is recorded and Δt is the time for the scan to progress from the center to the edge. Thus,

$$\theta = \arcsin\left(r/R\right) = \arcsin\left[\left(t - t_0\right)/\Delta t\right] \tag{6}$$

or by Pythagoras' theorem

$$\cos\left(\theta\right) = \sqrt{1 - \left(t - t_0\right)^2 / \Delta t^2} \tag{7}$$

The same angle θ appears in Eq. (5) and Eq. (7); hence,

$$I \;=\; I_0\left(\frac{2}{5} + \frac{3}{5}\sqrt{1 - \left(t - t_0\right)^2 / \Delta t^2}\right) \tag{8}$$

The solid and dashed lines in Figure 5 represent least squares fits to the limb darkening profile, which can be used to determine the mid-point of the scan and the extent of the solar disk. The Eddington approximation for a plane parallel atmosphere gives a reasonably accurate account of the data. The solid line in Figure 5 is an improved fit based on measurements of Pierce & Waddell (1961). By comparing the measured transit time with that predicted using the apparent solar diameter from the JPL Horizons ephemeris (http://ssd.jpl.nasa.gov) students investigate how close the observed chord is to a solar diameter.

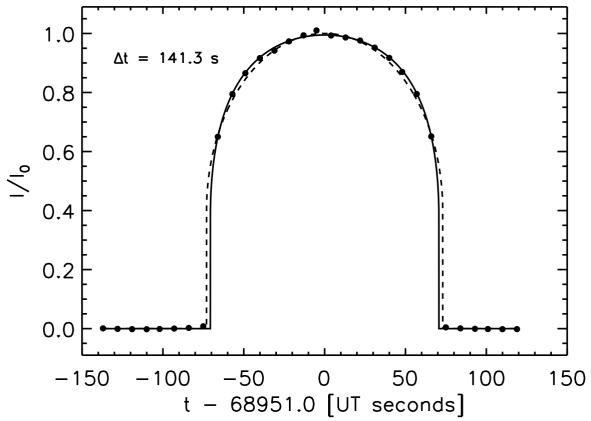

Figure 5: Total intensity versus time (UT seconds on 2008 December 22). The dashed line shows a least squares fit to the limb darkening in the Eddington approximation for a grey, plane-parallel atmosphere. The solid line shows to the limb darkening function of Pierce & Waddell (1961) at 630 nm. The mid point is 68951.0±0.3 s and the duration is 141.3±0.8 s. The predicted transit length on this date is 141.7 s; thus, the observed scan is consistent with one that cuts the sun at a diameter.

Figure 6 shows a small section of the first and last spectra from the scan displayed in Figure 5. The Doppler signature is evident—the absorption features in the first spectrum are systemically red-shifted relative to those in the last spectrum. This

figure provides a graphic demonstration of the small magnitude of the shift and that each absorption line contributes information regarding the Doppler shift.

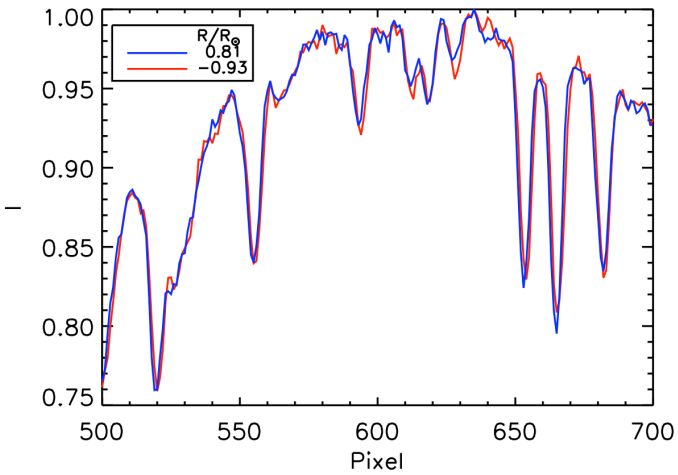

Figure 6: A small section (2.6 nm centered at 632.8 nm) of the solar spectra from the scan shown in Figure 5. The rotational Doppler shift is barely discernable between the first spectrum obtained at a projected radius of –0.93 $R_\odot$ (eastern redshifted solar limb) and the last 0.81 $R_\odot$ (western blueshifted solar limb).

References

Barden S.C., 1995, in Fiber Optics in Astronomical Applications, SPIE Proc. 2476, p. 2
Pierce, A. K.; Waddell, J. H. 1961 Memoirs Royal Astron. Soc., Volume 63, p. 89-112